Author's Version

Effect of pre-oxidation on cyclic oxidation resistance of γ-TiAl at 900 °C

R. Swadźba[a,1], Nadine Laska[2], Peter-Philipp Bauer[2], H. Krztoń[1]

[1]Łukasiewicz Research Network - Institute for Ferrous Metallurgy, Gliwice, Poland

[2]DLR German Aerospace Center, Cologne, Germany

[a]Corresponding author

Email address: rswadzba@gmail.com

KEYWORDS: γ-TiAl, High Temperature Oxidation, Intermetallics

ABSTRACT

The paper presents the effect of pre-oxidation on the high temperature oxidation behavior of γ-TiAl alloy. The pre-oxidation treatments were performed at 900 °C for 2 hours under various O and Ar mixtures which resulted in the formation of very thin (200-300 nm) oxide scales and oxygen enriched subsurface layers, containing the α_2-$Ti_3Al(O)$ and the $Ti_5Al_3O_2$ Z-phase. It is revealed that the pre-oxidation treatment can lower the oxidation rate of the alloy up to 300 hours. Detailed high resolution STEM investigations were performed to characterize the oxide scales and metal-scale interfaces.

1. Introduction

γ-TiAl alloys have been successfully applied for low pressure turbine blades over the past decade by major aircraft engines manufacturers such as General Electric and Pratt & Whitney [1–3]. Due to their excellent properties such as low density and high specific strength these materials are considered as a lighter alternative for the conventionally applied Ni-based superalloys. Their further development can provide improvements such as reduction of engine weight as well as an increase in its performance an efficiency [4,5].

Typically γ-TiAl alloys are capable of forming protective alumina scales upon exposure in pure oxygen up to 1000 °C [6]. However, oxidation in air results in reaction of TiAl with nitrogen leading to formation of TiN/Ti_2A1N layers at the metal-scale interface (nitrogen effect) [7–11] which limits their application to temperatures around 750 - 800 °C [4]. Since these nitrides are readily oxidized upon further high temperature exposure the resulting oxide scales that typically form on TiAl alloys are complex and consist of two main layers - an outer layer of TiO_2 which grows by outward diffusion of interstitial Ti ions and an inner layer of TiO_2 + Al_2O_3 mixture growing by inward oxygen diffusion [4,12]. Such intermixed layers are considered to be protective to about 800 °C above which the oxidation resistance of the γ-TiAl alloys decreases rapidly. It is related to the fact that TiO_2 has a much higher growth rate than Al_2O_3 and it doesn't act as an efficient diffusion barrier for interstitials such as oxygen and nitrogen that embrittle the alloy leading to deterioration of its mechanical properties [4]. This is mainly caused by the very high solubility of oxygen in the α_2 and γ phases which is 12-15 at. % and 3 at. %, respectively [13].

In order to improve the high temperature performance of γ-TiAl alloys numerous coating solutions have been investigated in the past that include application of such technologies as PVD [14–19], vapor phase aluminizing [20–22], pack cementation [23], slurry aluminizing [20,24] or halogen effect [25–28]. Other treatments such as pre-oxidation have been shown to reduce the oxidation rate of TiAl alloys thus prolonging the lifetimes of these materials under high temperature conditions. The beneficial effect of pre-oxidation is that a protective scale, which can be maintained, but not initiated in air, is established during heat treatment under a controlled atmosphere [29–31]. Additionally, the application of pre-oxidation is mandatory for the application of a Thermal Barrier Coating (TBC) on γ-TiAl which in the future will allow for the reduction of base metal temperature and therefore increase its lifetime. The formation

of a very thin and adherent alumina scale is necessary to provide a good bonding between the outer ceramic top coat and the metal substrate [17,21,27,32].

This paper concerns the influence of pre-oxidation treatment under atmospheres containing various amounts of oxygen on the cyclic oxidation resistance of TiAl alloy at 900 °C. Detailed microstructural investigations using Scanning Transmission Electron Microscopy (STEM) were performed in order to characterize the growth of the initially formed oxide scale as well as the oxygen enriched subsurface layer and their further evolution during high temperature exposure.

2. Experimental Procedure

The base material was the 48-2-2 TiAl alloy provided by GfE GmbH from Germany containing 48% Al, 2 % Cr, 2% Nb (all in atomic %) and balance Ti. The alloy was cast to an ingot with 80 mm of diameter from which bars with diameter of 15 mm were cut using Electro Discharge Machining (EDM) method. The bars were then cut to coupons with thickness of 2 mm and EDM was used to drill holes with diameter of around 1.8 mm for hanging purposes. The coupons were polished to 3 μm surface finish and subject to pre-oxidation treatment. The pre-oxidation experiments were performed in a Carbolyte furnace at 900 °C for 2 hours under 1 bar pressure in three atmospheres that included 0.01% O_2 + Ar, 1% O_2 + Ar and 100% O_2 (all in vol. %). The samples were subject to the cyclic oxidation test at 900 °C in 1 hour cycles and their weight was measured using an analytical balance after every 50 cycles up to 1000 cycles. After every cycle the samples were cooled in ambient air for 15 minutes. The surface and cross-sectional microstructure investigations of the samples were performed using a Scanning Electron Microscope (SEM) JEOL JSM 7200F equipped with Energy Dispersive Spectrometer (EDS) and Electron Backscatter Diffraction Detector (EBSD) by EDAX as well as a Field Emission Gun (FEG) operated at 15 kV. The microstructures of the oxide scales as well as subsurface layers were investigated using high resolution Scanning Electron Microscopy

(STEM) using FEI TITAN 80-300 equipped with EDS and an X-FEG operated at 300 kV. The samples for STEM investigations were prepared using Focused Ion Beam (FIB) method on FEI Quanta 3D 200i SEM. In this process platinum layers were deposited on the surface of the investigated samples to protect them from gallium ion (Ga^+) damage. The phase composition at elevated temperatures, up to 900 °C, was studied using Bruker D8 Advance system equipped with a high temperature chamber HTK 1200N by Anton Paar utilizing a copper tube.

3. Results and Discussion

3.1. Characterization of the microstructure and initial stages of oxidation of the investigated γ-TiAl material

The SEM-BSE image of the investigated γ-TiAl alloy along with its phase composition analysis using EBSD are shown in Fig. 1a-c. As evidenced in the EBSD orientation (Fig. 1b) and phase maps (Fig. 1c) the alloy's microstructure is characterized by the presence of massive γ-TiAl grains around 100 µm in size along with elongated α_2-Ti_3Al as well as blocky β-Ti grains. Quantitative XRD analysis using Rietveld method revealed that the alloy contains 92,8 vol.-% ± 0,2 γ-TiAl, 3,3 vol.-% ± 0,1 α_2-Ti_3Al as well as 3.9 vol.-% ± 0,1 β-Ti phase.

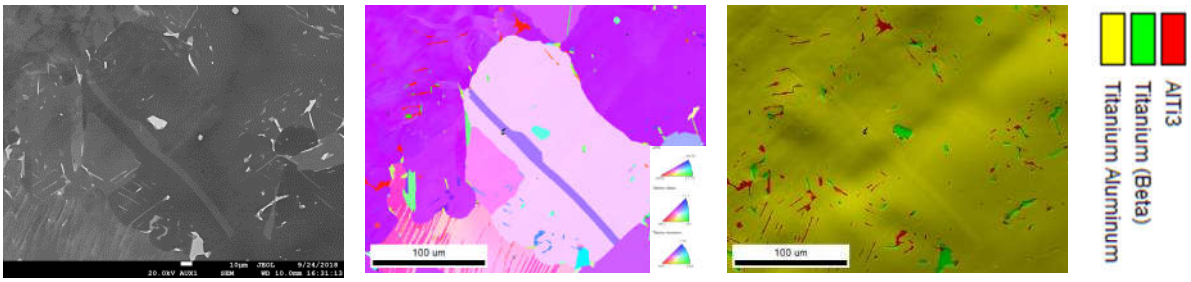

a) b) c)

Fig. 1. Microstructure of the investigated γ-TiAl alloy: SEM-BSE (a), EBSD orientation map (b) and c) EBSD phase map.

In order to characterize and demonstrate the differences between the initial stages of oxidation in air and in oxygen the high temperature X-ray diffraction (HT-XRD) experiment

was performed on bare TiAl with surface finish of 3 μm. The phase composition of the sample was measured at room temperature, after heating in air up to 900 °C and in 15 minutes intervals up to 60 minutes at 900 °C as well as after cooling back to room temperature. The assembly of corresponding diffractograms is presented in Fig. 2. The obtained results indicate that at room temperature only the γ-TiAl phase is present. Upon heating to 900 °C the peaks of TiO_2 can be clearly distinguished indicating the onset of surface oxidation. During the next 15 minutes at 900 °C first peaks of TiN as well as α-Al_2O_3 appeared. Further measurements after 30, 45 and 60 minutes at 900 °C show increasing signals from both these phases caused by reaction of the alloy with N and O with simultaneous formation of titania. The results of the HT-XRD measurements allowed to characterize the initial stages of oxidation of the untreated TiAl in air and were in agreement with literature data concerning the "nitrogen effect" where oxidation in air results in formation of intermixed TiN and Al_2O_3 scales preventing the development of a continuous alumina layer and facilitates the formation of rapidly growing and non-protective mixed titania and alumina scales. Since these oxide layers are permeable to nitrogen its continuous supply will form Ti and Ti-Al nitrides with the substrate alloy, that readily oxidize upon further high temperature exposure [11,33,34] and maintain the accelerated oxidation kinetics [10].

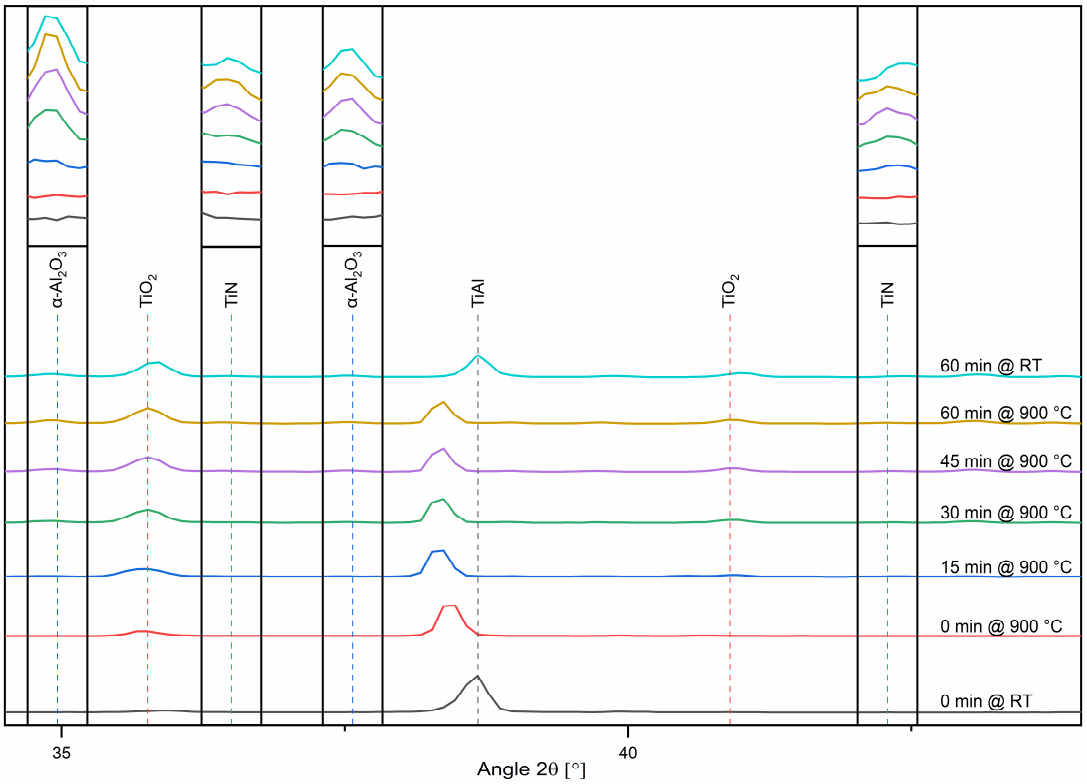

Fig. 2. High temperature XRD diffractograms obtained for bare TiAl sample with 3 µm finish between room temperature and 900 °C in air. The upper part of the image shows the magnification of the selected peaks.

3.2. Pre-oxidation experiments at 900 °C for 2 hours under various atmospheres

The images shown in Fig. 3a-c represent the γ-TiAl coupons that were subject to pre-oxidation treatments at 900 °C for 2 hours under atmospheres containing various amounts of of oxygen and argon. These include 0.01 % O_2 + Ar (Fig. 3a), 1% O_2 + Ar (Fig. 3b) and 100% O_2 (Fig. 3c). The surface morphologies obtained during pre-oxidation experiments under all atmospheres were similar, i.e. characterized by a dull, gray shade with numerous yellow areas. In case of all atmospheres used in pre-oxidation treatments the whole surface of the samples was uniformly oxidized to a mixture of needle-shaped and nodule-like oxides, as shown in Fig. 3a-c. Based on XRD results it was shown that these oxides include TiO_2 and α-Al_2O_3 (Fig. 3g).

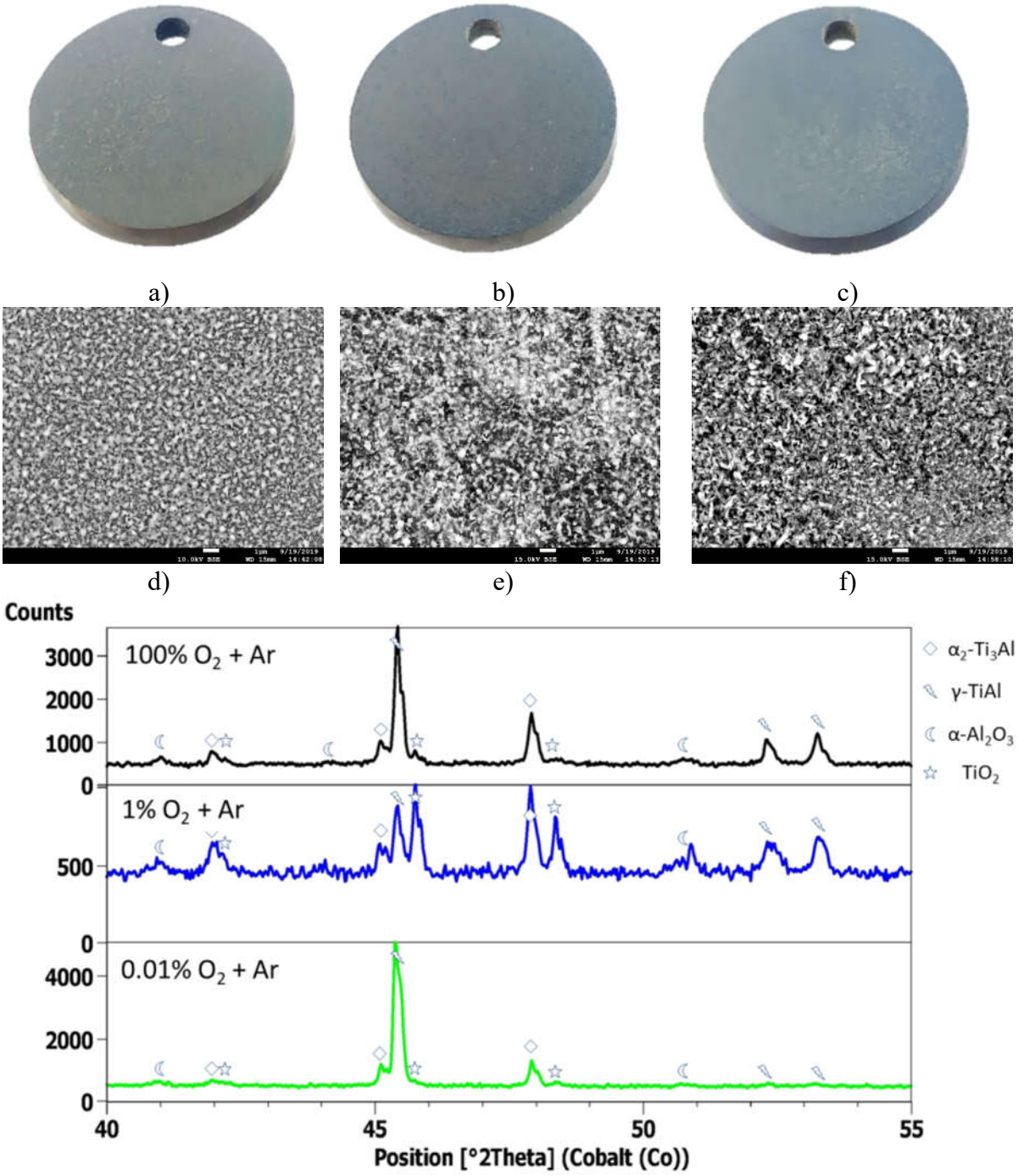

Fig. 3. Coupons made of the investigated γ-TiAl alloy along with SEM-BSE images of surface microstructures after preoxidation at 900 °C for 2 hours under a,d) 0.01% O_2 + Ar, b,e) 1% O_2 + Ar and c,f) 100% O_2 + Ar as well as phase composition XRD diffractograms (g).

In order to study the effect of pO_2 on the initial oxide scale growth and subsurface evolution during pre-oxidation systematic STEM investigations were performed on the metal scale interfaces. The cross-sectional STEM-HAADF images of metal-scale microstructures formed during pre-oxidation treatments in 0.01% O_2, 1% O_2 and 100% O_2 atmospheres are shown in Fig. 4a-c.

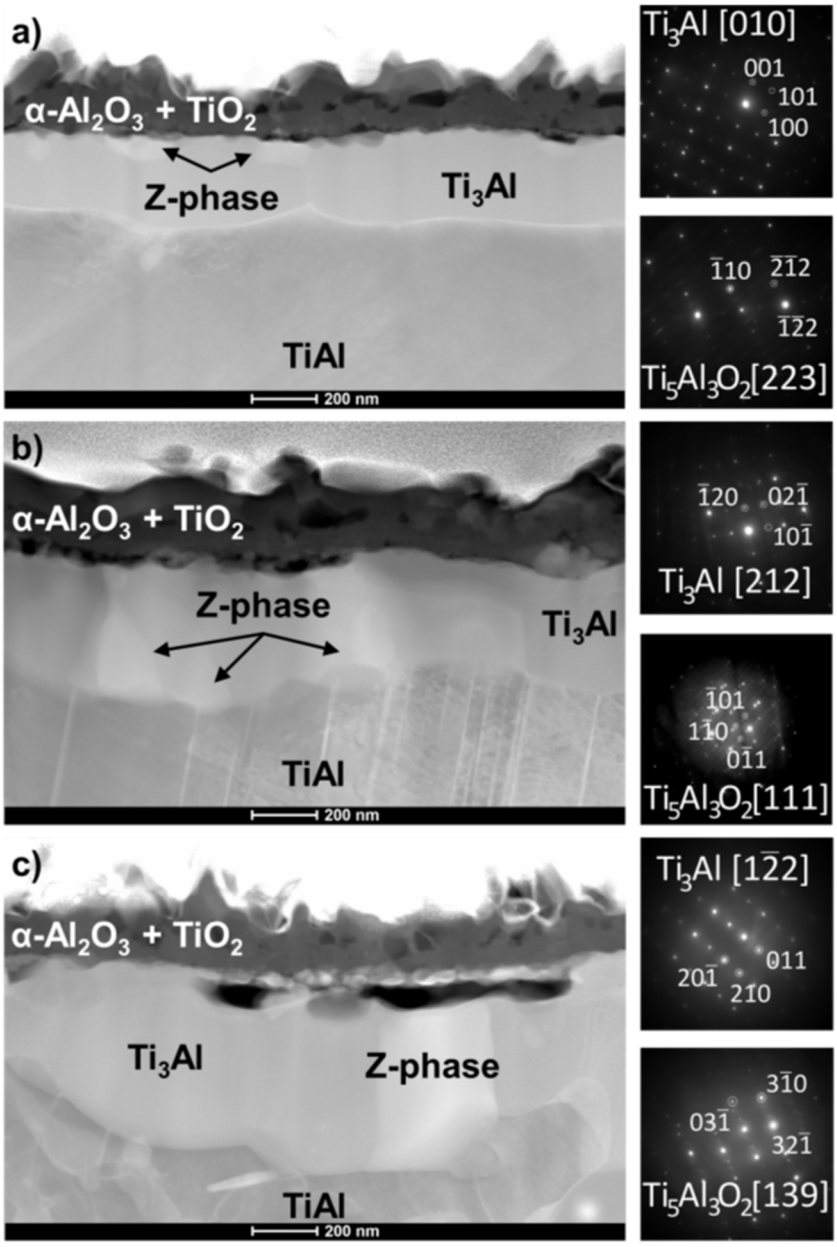

Fig. 4. Cross-sectional STEM-HAADF images of the oxide scale and subsurface layer formed on the investigated γ-TiAl alloy after pre-oxidation at 900 °C for 2 hours under a) 0.01% O_2 + Ar, b) 1% O_2 + Ar and c) 100% O_2 + Ar.

The performed investigations revealed that the effect of oxygen concentration in the atmosphere on the metal-scale microstructure is two-fold. Firstly, increasing the amount of oxygen leads to an increase in oxide scale thickness. After pre-oxidation in 0.01% O_2 + Ar atmosphere the oxide scale thickness is around 160 nm (Fig. 4a). With the increase of oxygen concentration to 1% the observed oxide scale thickness increases to 240 nm (Fig. 4b), while in the case of 100% oxygen content it is between 200 and 290 nm (Fig. 4c).

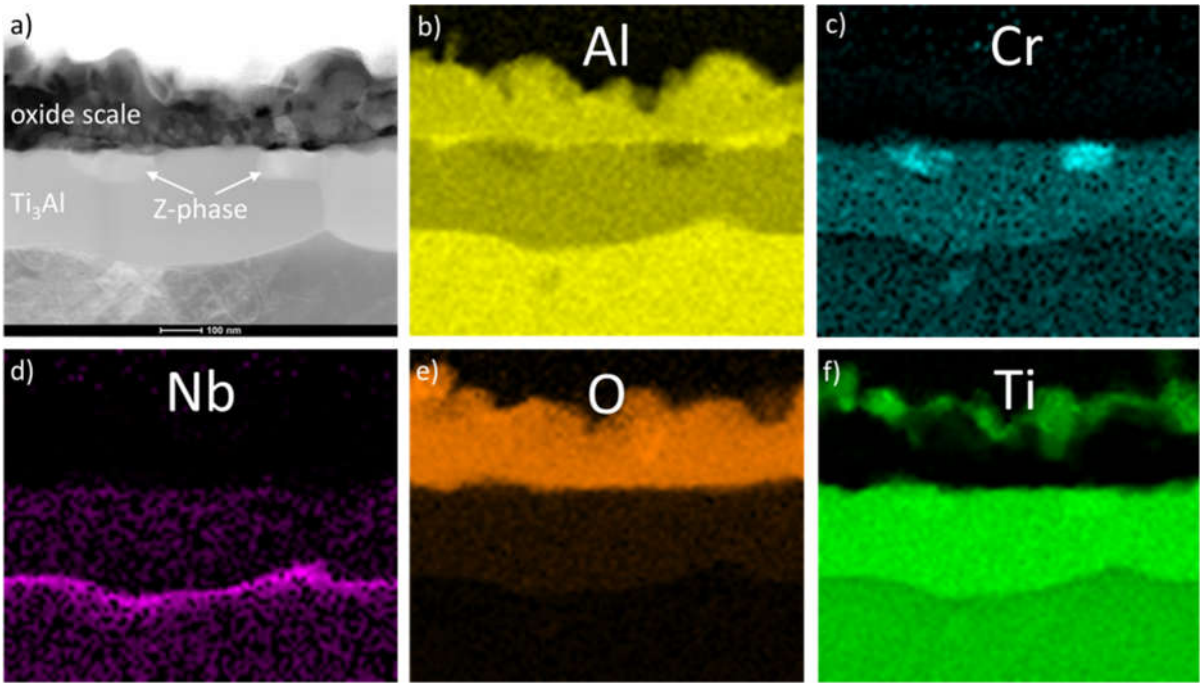

Fig. 5. STEM-EDS elemental distribution images of the oxide scale and subsurface layer formed on the investigated γ-TiAl alloy after preoxidation at 900 °C for 2 hours under 0.01% O_2 + Ar atmosphere (a), b) Al, c) Cr, d) Nb, e) O and f) Ti.

The elemental mappings performed in the metal-scale interface area shown in Figs. 5-7 indicate that the formed oxide scales consist of two zones in all cases. The outer very thin zone contains Ti and O which in combination with XRD results can be identified as TiO_2 while the inner zone is most certainly α-Al_2O_3. It is noteworthy that in the case of all three pre-oxidation treatments the outer TiO_2 layer is completely isolated from the metal by the continuous alumina oxide scale. In addition to the differences in oxide scale thicknesses the concentration of oxygen

in the atmosphere during pre-oxidation at 900 °C also influences the subsurface layer in the metal substrate.

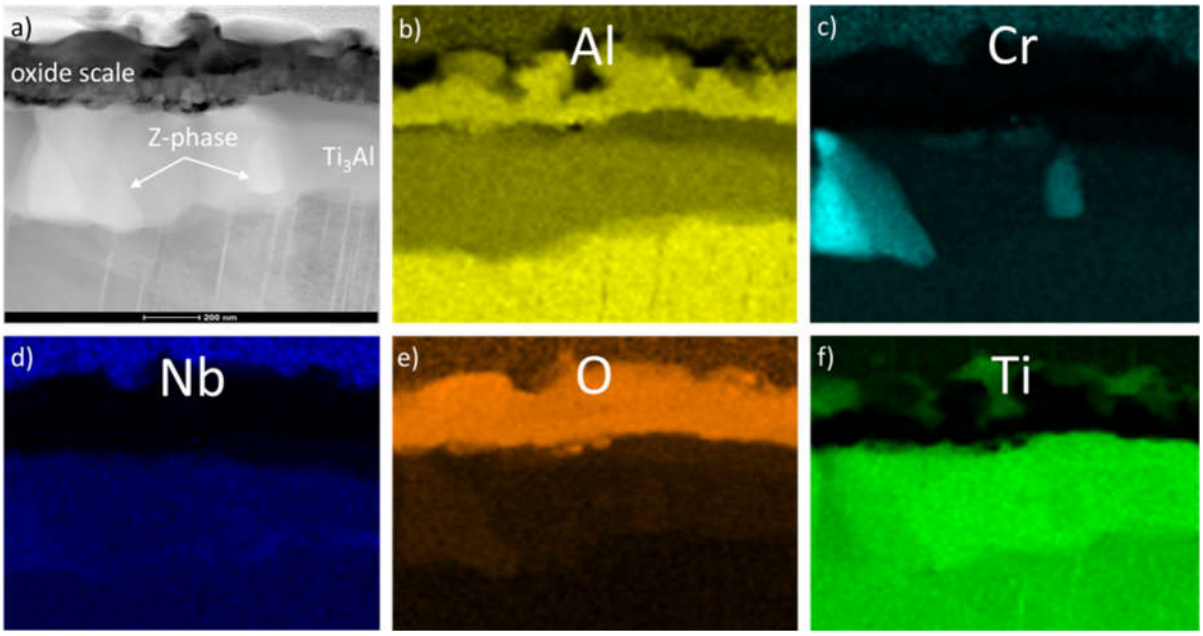

Fig. 6. STEM-EDS elemental distribution images of the oxide scale and subsurface layer formed on the investigated γ-TiAl alloy after preoxidation at 900 °C for 2 hours under 1% O_2 + Ar atmosphere (a), b) Al, c) Cr, d) Nb, e) O and f) Ti.

As shown in elemental mappings in Figs. 5, 7 and 8 between the oxide scales and the TiAl substrate an additional zone was formed that contained an increased content of Ti, O and Cr. Simiarly to the oxide scale this oxygen enriched zone is also thicker in case of pre-oxidation processes performed in atmospheres containing higher amounts of oxygen. As a matter of fact, this dependency is even more pronounced compared to oxide scale thickness. After pre-oxidation in 0.01% O_2 + Ar the O-rich zone is around 280 nm thick, while in 1% O_2 + Ar and 100% O_2 it is 460 and 590 nm thick, respectively. The STEM-EDS elemental mappings shown in Figs. 5-7 also indicated that there are additional grains in the O-rich subsurface zone that contain an increased content of Cr. Based on electron diffraction investigations the matrix of the O-rich zone was identified as α_2-Ti_3Al phase enriched in oxygen while these Cr-enriched precipitates were found to be the $Ti_5Al_3O_2$ phase, also named as Z-phase in the literature

[13,34,35]. The Z-phase grains were observed for all samples, however their amount and size increases significantly with increasing the oxygen concentration in the atmosphere during pre-oxidation. As a matter of fact in the case of pre-oxidation in 0.01% O_2 + Ar there are only 2-3 grains visible in the field of view (Fig. 4a) and they are present at the metal-scale interface only. Increasing the oxygen content in the atmosphere led to formation of large grains that reach from the substrate metal up to the oxide scale (Fig. 4b,c).

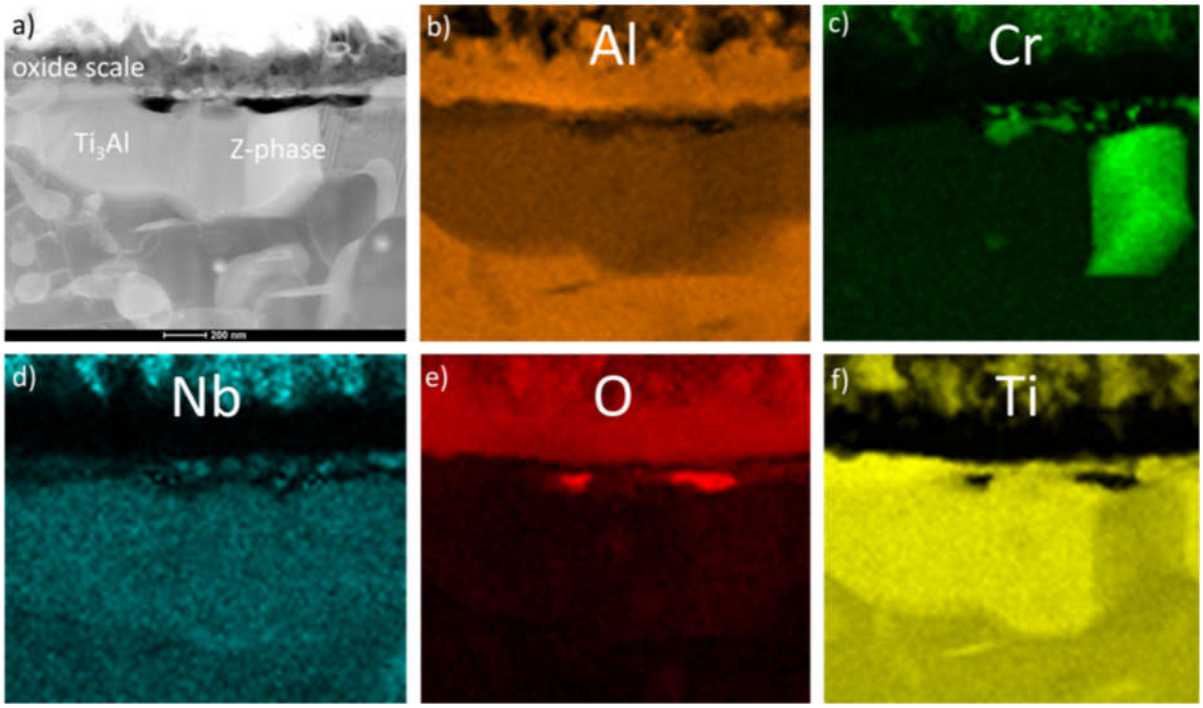

Fig. 7. STEM-EDS elemental distribution images of the oxide scale and subsurface layer formed on the investigated γ-TiAl alloy after preoxidation at 900 °C for 2 hours under 100% O_2 + Ar atmosphere (a), b) Al, c) Cr, d) Nb, e) O and f) Ti.

3.3. Cyclic oxidation test at 900 °C in air

The results of the cyclic oxidation test performed at 900 °C up to 1000 1 hour cycles are shown in form of mass change curves as a function of the number of 1 h cycles in Fig. 8.

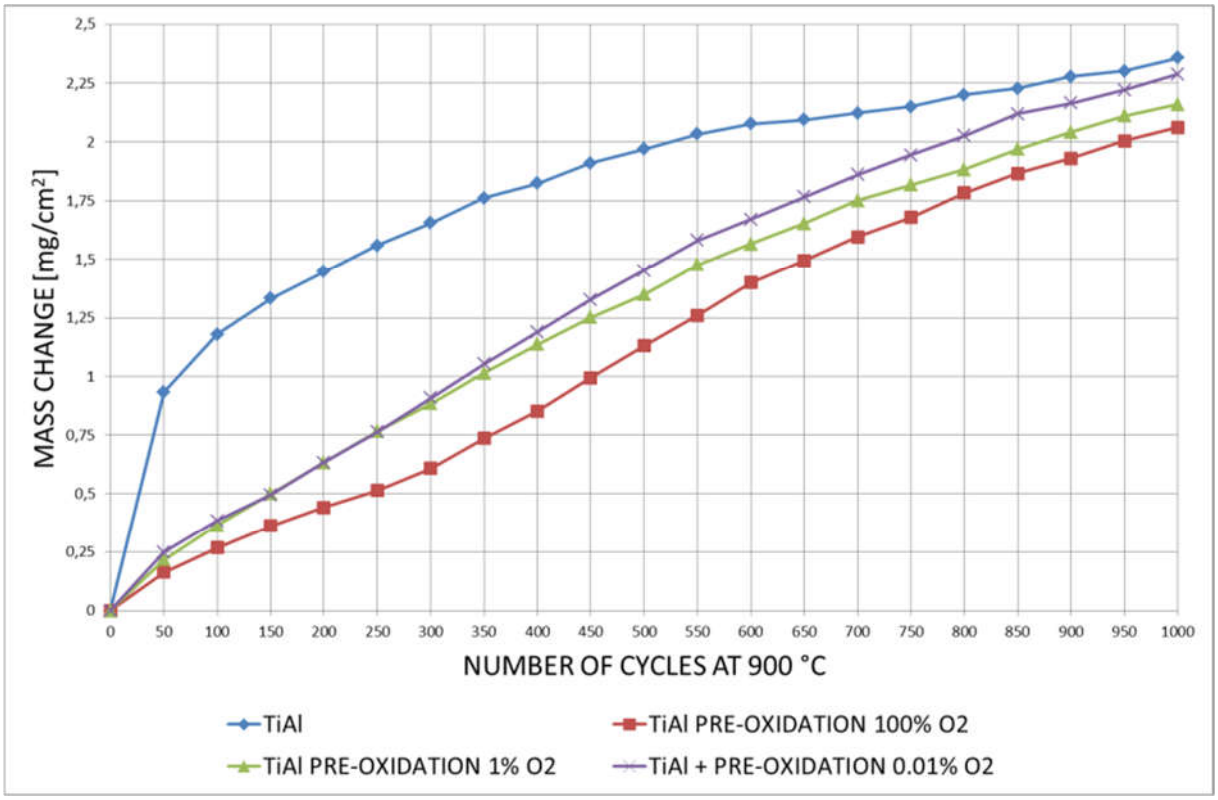

Fig. 8. Mass change curve of γ-TiAl without treatment and after pre-oxidation at 900 °C for 2h under 0.01%, 1% and 100% O_2 + Ar.

The effect of pre-oxidation on the mass change of all the samples is clearly visible during the initial several hundred hours of oxidation. The untreated TiAl sample exhibited a rapid mass gain during the first 50 cycles almost up to 1 mg/cm^2 and then oxidized according to the cubic law up to over 2,35 mg/cm^2 after 1000 cycles. The pre-oxidized samples also exhibited a parabolic oxidation behavior however their mass gains were significantly lower compared to untreated TiAl. Moreover, a difference in the mass gains was observed depending on the atmosphere of pre-oxidation treatment. The lowest mass gain was observed for the coupon pre-oxidized in 100% O_2 which is especially visible during the first 300 hours where the difference between the pre-oxidized sample and untreated alloy is equal to 1 mg/cm^2. After this period of oxidation the mass change increases considerably faster up to over 2 mg/cm^2 which is also lower than that for the untreated alloy. What is more, the mass change for the coupons pre-oxidized in 0.01% and 1% O_2 is similar during the first 300 cycles but still higher than that of the coupon pre-oxidized in 100% O_2. Between 300 and 1000 cycles the coupon pre-oxidized in

higher O_2 content exhibits a mass gain between that for the samples pre-oxidized in 100% and 0.01% O_2.

In order to study the oxidation behavior of the studied samples with pre-oxidation treatment and without it additional mass change curves were prepared (Fig. 9). In these curves the squared mass gain is presented as a function of oxidizing time in hours (equivalent to the number of cycles) thus allowing to calculate the parabolic rate constants - kp in $mg^2cm^{-4}h^{-1}$. It can be seen that the oxidation behavior of untreated TiAl (Fig. 9a) differs significantly from that of the pre-oxidized samples (Fig. 9b-d). It exhibits two stages of oxidation where the first one is characterized by a higher parabolic rate constant $kp = 6{,}16 \cdot 10^{-3}$ $mg^2cm^{-4}h^{-1}$ and lasts up to around 550 hours of exposure. After this time the oxidation rate decreases almost twice to $kp = 3{,}32 \cdot 10^{-3}$ $mg^2cm^{-4}h^{-1}$. All the pre-oxidized samples also exhibit two stages of oxidation where during the first 200 – 300 hours the parabolic rate constant is significantly reduced compared to second stage which lasts for the remaining several hundred hours up to 1000 hours. During the first stage the parabolic rate constant was observed to be the highest ($2{,}36 \cdot 10^{-3}$ $mg^2cm^{-4}h^{-1}$) for the sample pre-oxidized in 1% O_2 + Ar atmosphere, while it pre-oxidation performed under 100% O_2 led to the lowest kp – $1{,}35 \cdot 10^{-3}$ $mg^2cm^{-4}h^{-1}$. Moreover, pre-oxidation in atmospheres containing low amount of oxygen, i.e. 0.01% and 1%, led to a shorter period of reduced oxidation rate which was around 200 hours. On the other hand, pre-oxidation in pure oxygen allowed maintaining the lowered oxidation rate up to 300 hours. After this time the oxidation kinetics of all the pre-oxidized samples increased to a value of around $5{,}67 – 6{,}41 \cdot 10^{-3}$ $mg^2cm^{-4}h^{-1}$ which is comparable to that of untreated TiAl alloy during the first oxidation stage. This state was maintained up to 1000 hours of oxidation and no other changes in oxidation kinetics were observed during this time.

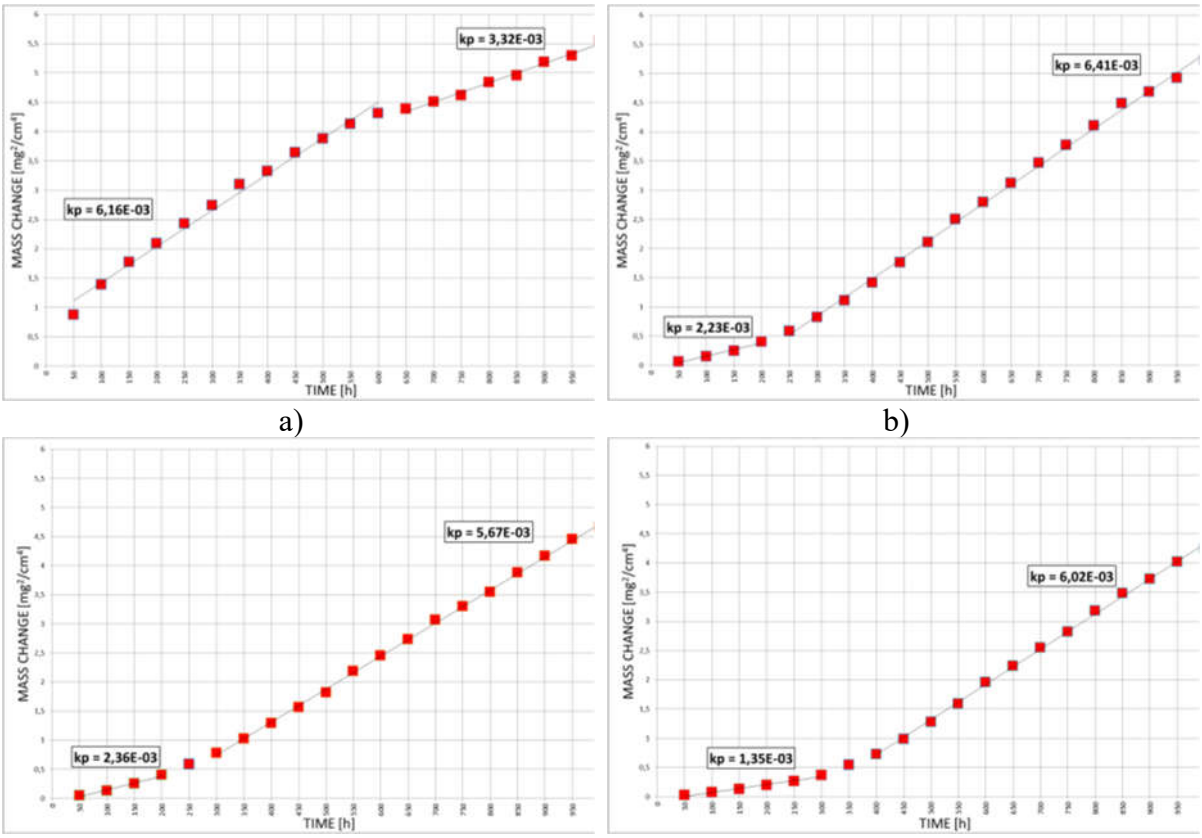

Fig. 9. Determination of parabolic rate constant *kp* for γ-TiAl without treatment (a) and after pre-oxidation at 900 °C for 2h under b) 0.01% O_2 + Ar, c) 1% O_2 + Ar and d) 100% O_2 + Ar.

The visual appearance of TiAl coupons after various treatments and subsequent cyclic oxidation test at 900 °C up to 1000 cycles is shown in Fig. 10 along with SEM investigations results of the surface and cross-sectional microstructures.

After the cyclic oxidation test all the samples, both untreated and pre-oxidized under various atmospheres, were characterized by a yellow color indicative of titania formation on their whole surface. Based on the XRD results shown in Fig. 11, the oxide scales that formed during the cyclic oxidation test were found to be mostly titania and alumina. The surface appearance as well as phase composition of the pre-oxidized samples is comparable to the untreated one after 1000 cycles at 900 °C (Fig. 10a-d). The differences can be observed in the surface microstructure where the untreated sample and the pre-oxidized one under 0.01%

O_2 + Ar are completely covered with titania nodules (Fig. 10a,b). On the other hand, the samples pre-oxidized under atmospheres with higher oxygen content, i.e. 1% and 100% O_2, exhibit a mixed oxide scale microstructure on the surface after the cyclic oxidation test. As a matter of fact, numerous areas containing a majority of alumina were found as shown in Fig. 10c,d. Whether these regions are present due to scale spallation and healing or because the formation of titania was hindered by pre-oxidation is presently unknown. The cross-sectional microstructure of the oxide scale formed on untreated TiAl contains a typical outer titania layer undercut by alumina and titania mixture with majority of alumina as well as titania and alumina mixture at the interface with the substrate. The oxide scales formed on pre-oxidized samples after the cyclic oxidation test are very similar in terms of thickness and phase composition, however a subtle difference between them and the untreated TiAl sample can be observed underneath the outer titania layer. As shown in Fig. 10b-d the layer underneath the outer titania layer is not a mixture of titania and alumina, as it is observed in Fig. 10a for untreated TiAl, but it is composed solely of a very thin layer of pure alumina. In fact it is believed to be the alumina layer formed during the pre-oxidation treatment. Upon subsequent cyclic oxidation test it was embedded in the oxide scale that grew by inward oxygen diffusion as well as by outward Ti^{4+} diffusion. It is evidenced by the fact that the outer titania layer thickened significantly compared to its initial state after pre-oxidation while beneath the initially formed alumina layer a mixture of titania and alumina formed.

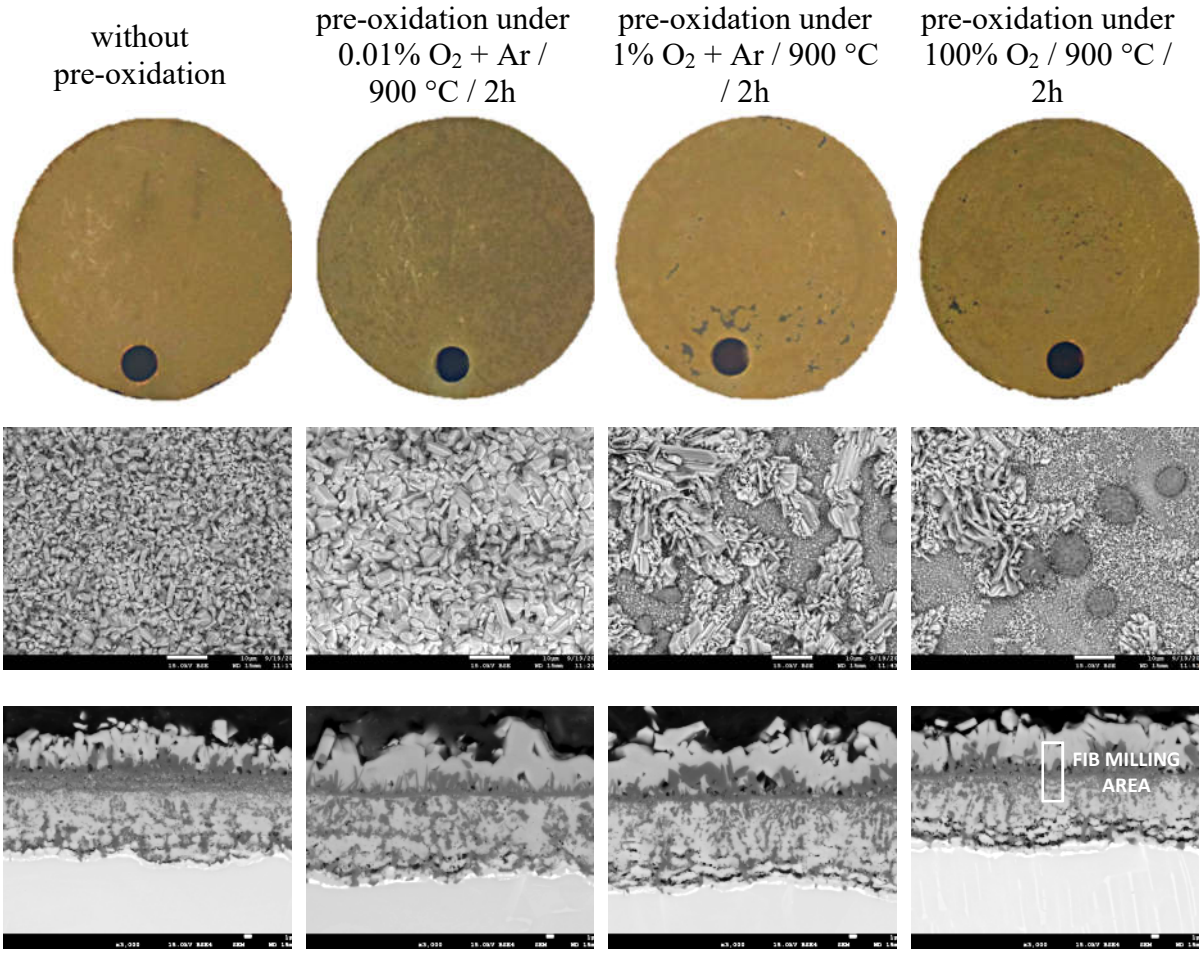

Fig. 10. Visual appearance of γ-TiAl along with surface and cross-sectional microstructures of coupons after the cyclic oxidation test up to 1000 1h cycles at 900 °C: a) without pre-oxidation and after pre-oxidation in b) 0.01% O_2 + Ar / 900 °C / 2h, c) 1% O_2 + Ar / 900 °C / 2h and d) 100% O_2 / 900 °C / 2h.

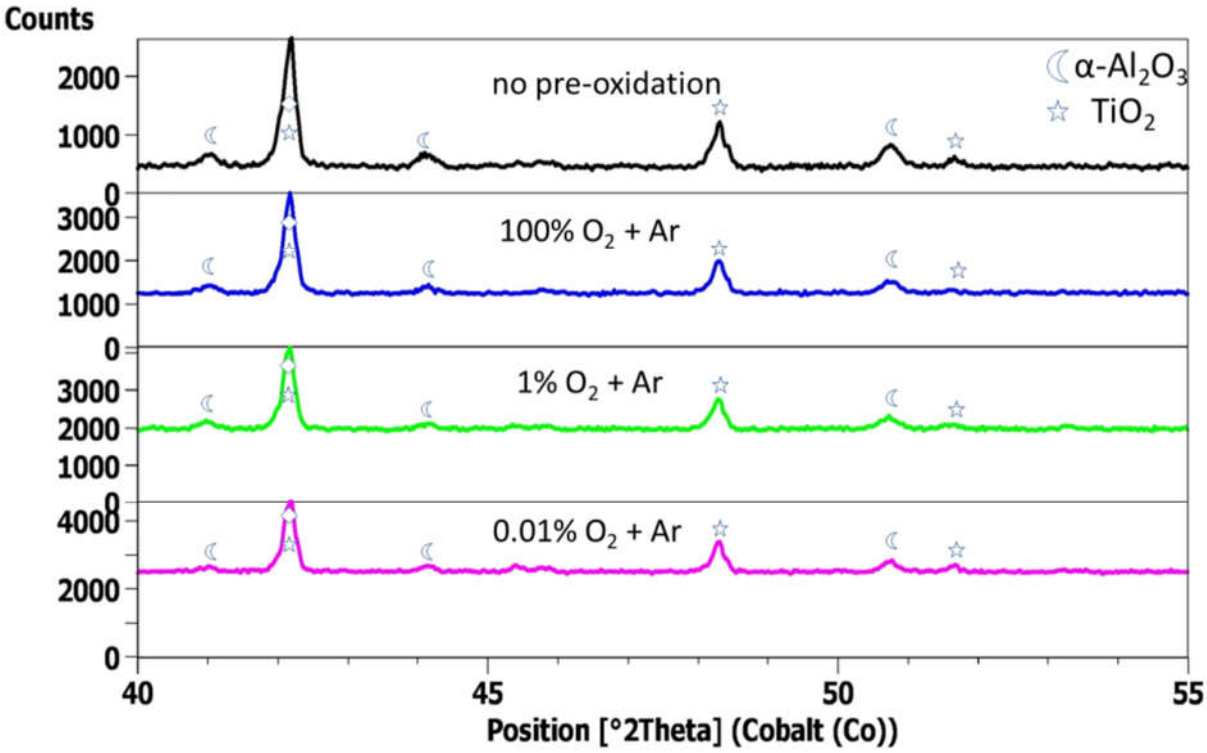

Fig. 11. XRD results of all the investigated samples after the cyclic oxidation test.

4. Discussion

The performed pre-oxidation experiments allowed evaluating the effect of gas atmosphere, i.e. on the growth of the initial oxide scale and subsurface layer, as well as the further high temperature oxidation behavior of the investigated TiAl alloy. The application of pre-oxidation at 900 °C for 2 hours under controlled atmosphere containing a mixture of argon and oxygen or solely pure oxygen allowed for the formation of very thin (200-300 nm), continuous and adherent oxide scales composed in majority of α-alumina. Other research works that involved pre-oxidation treatment of TiAl alloys assumed that preferential oxidation of aluminum occurring under very low oxygen partial pressures provides significant improvement in oxidation resistance of TiAl alloys. Taniguchi et al. [30,31,36,37] studied the effect of various pre-oxidation experiments that involved burying the samples in rutile, silica or chromia/chromium powders to provide very low pO_2. These experiments were performed at around 927 °C (1200 K) for over 27 hours (100 ks) and provided measurable improvement during the cyclic oxidation testing at 1026 °C (1300 K) [30,31,36,37]. Other research works

involved lower temperatures but longer pre-oxidation times [38] that also improved the high temperature oxidation resistance of TiAl. The results of this study indicate that application of a relatively short time (2 hours) of pre-oxidation at 900 °C in oxygen or its mixture with argon allows to form an adherent and continuous alumina scale which is effective for several hundred hours of oxidation at 900 °C. Compared to oxidation in air, the pre-oxidation treatment in pure oxygen or its mixture with argon makes it possible to effectively eliminate nitrogen from the atmosphere during the initial stages of the oxide scale growth. As shown in the STEM results such scales are mostly composed of alumina along with the subsurface formation of the Z and $Ti_3Al(O)$ phases.

The formation of nanometric titania precipitates within the outer layer of the oxide scale observed for all pre-oxidation treatments performed in this study can be related to the surface finish of the studied samples. As a matter of fact it has been shown previously ground TiAl show the ability to form a continuous and protective Al_2O_3 scales whereas on smooth surfaces a rapidly growing TiO_2 and Al_2O_3 mixtures form [39]. It is noteworthy that this initially formed titania layer was completely undercut by alumina scale which became rate controlling during further high temperature oxidation.

It has been shown that the pre-oxidation treatment performed under 100% O_2 allows to provide the lowest oxidation kinetics ($k_p = 1.35 \cdot 10^{-3}$ $mg^2cm^{-4}h^{-1}$) among all the three investigated atmospheres for the longest time, i.e. around 300 hours. After this period the protectiveness of the initially formed oxide scale is lost and the oxidation kinetics increase to values very similar to those observed for untreated TiAl alloy. The further evolution of the oxide scale involves the thickening of the outer titania layer as well as formation of a non-protective titania and alumina mixture along with a continuous layer at the metal-scale interface, which most likely contains Ti and Ti-Al nitrides [9,10,40]. While the latter phenomenon can be explained by the fact that both oxygen and nitrogen readily diffuse through the oxide scale [33]

and react with the substrate alloy the thickening of the outer titania layer requires outward diffusion of interstitial Ti ions [12]. In order to understand how Ti^{4+} is transported through the continuous preformed alumina layer additional high resolution STEM investigations were performed in the area marked in Fig. 10d. As shown in Fig. 12 after the cyclic oxidation test the initially protective alumina layer is somewhat thicker and more porous compared to its initial condition. However, the elemental mappings of Al and Ti (Fig. 12b,c) indicate that it is still a diffusion barrier separating the outer titania layer from the inner titania and alumina mixture. Based on the distribution of Ti (Fig. 12c) it can be observed that Ti is present only within the nanometric porosities of the alumina layer. It is also noteworthy that both Cr and Nb are present only in the inner mixture of titania and alumina and not within the outer titania layer. Based on the detailed microstructural analysis of the alumina layer shown in Fig. 13a it can be observed that it is very fine-grained. Moreover, the presented STEM-HAADF image which is sensitive to variations in the atomic number of elements (Z contrast) in the analyzed area indicates that the grain boundaries appear brighter indicating that additional elements are present in that area. As a matter of fact, STEM-EDS elemental mapping shown in Fig. 13b,c proves that both Ti and Cr are segregated to the grain boundaries of the alumina scale. This result clearly shows that these elements are transported from the metal to the gas atmosphere through the grain boundaries of the somewhat continuous and dense alumina layer.

Another important effect of pre-oxidation observed in this study is the formation of the oxygen enriched zone underneath the oxide scale. It has been demonstrated that increasing the concentration of oxygen in the atmosphere leads to thickening of this subsurface layer as well as alters its phase composition. In the 0.01% O_2 atmosphere this zone contains mostly the O-enriched α_2-Ti_3Al(O) phase with very fine Z-phase precipitates ($Ti_5Al_3O_2$) while after pre-oxidation under 100% O_2 the grains of the latter phase are much larger. Literature data indicates that this ternary compound (Z-phase) is in equilibrium with alumina rather than titania [33,35]

and its presence can be beneficial for oxidation resistance of TiAl alloy. While on binary alloys based on γ-TiAl phase it is possible to form a continuous Z-phase layer on other alloys containing the α_2 phase its formation is significantly hindered [41]. Moreover, with further exposure the Z-phase is also known to decompose to the α_2 phase which due to its high solubility of oxygen allows for internal aluminum oxidation as well as formation of titania and a strong increase in scale growth rate [13,33,41]. This transition from protective to non-protective oxidation is even more strongly enhanced by the of nitrogen present in the atmosphere [21,34]. The results obtained in this study are not completely in agreement with those findings since the performed investigations revealed that all the studied pre-oxidation conditions led to formation of oxygen enriched zone which was in majority the α_2-$Ti_3Al(O)$ with varying content (but still minor) of the Z-phase. Yet, the pre-oxidation treatment allowed reducing the oxidation kinetics for around 300 hours at 900 °C. It is thus concluded that this improvement is an effect of a synergy between the formed oxide scale and the subsurface O-enriched layer.

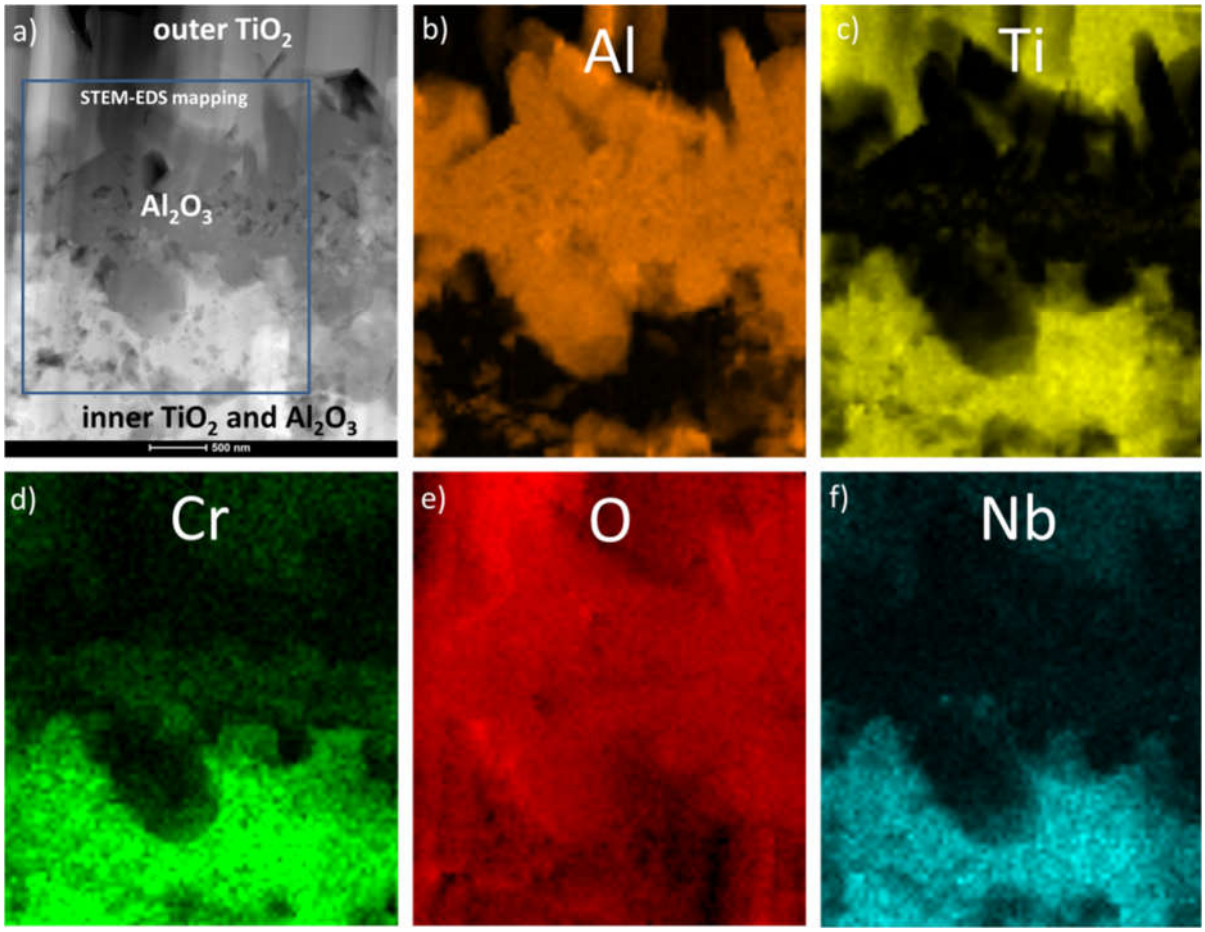

Fig. 12. STEM-HAADF image of the oxide scale marked in Fig. 9d (a) and elemental mappings of b) Al, c) Ti, d) Cr, e) O and f) Nb.

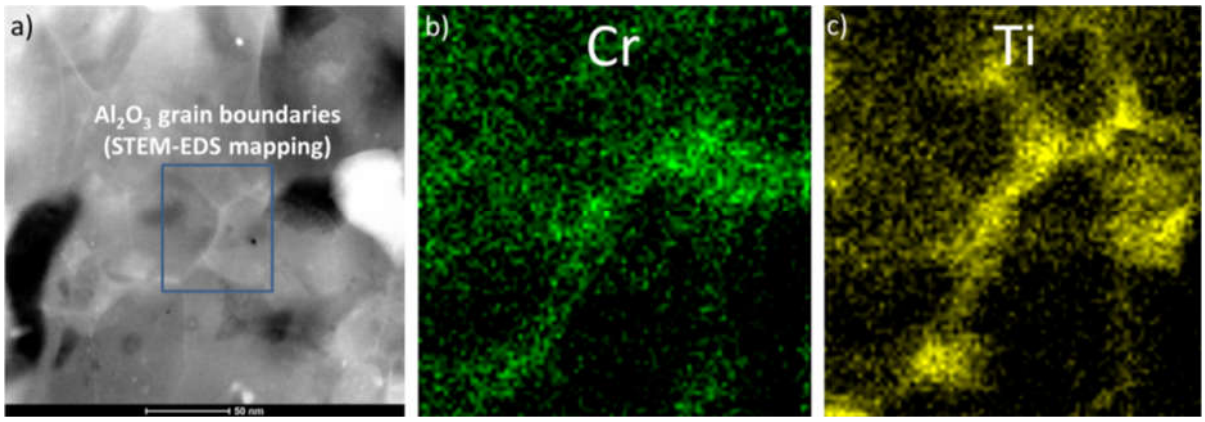

Fig. 13. STEM-HAADF image of the alumina oxide scale along with elemental mapping from the grain boundary (a) of b) Cr and c) Ti.

5. Summary

The high temperature oxidation resistance of TiAl alloy at 900 °C can be improved by application of pre-oxidation treatment at 900 °C for 2 hours in pure oxygen. The application of lower amounts of oxygen in this atmosphere is also beneficial, however, the observed oxidation kinetics are higher. The oxide scale formed in pure oxygen during the pre-oxidation treatment is composed of a very thin and continuous α-alumina oxide scale with a thickness of around 200 to 300 nm. Underneath the formed oxide scale an oxygen enriched subsurface layer is formed which is mostly composed of α_2-$Ti_3Al(O)$ phase with some Z-phase grains. The amount of the Z-phase increases with increasing the oxygen content in the atmosphere. Upon high temperature oxidation at 900 °C the formed α-alumina oxide scale provides a decrease in the oxidation kinetics for around 300 hours after which it increases to the level equivalent to the untreated TiAl alloy. This loss of protective properties is related to the outward grain boundary diffusion of Ti and inward diffusion of oxygen and nitrogen through the scale leading to formation of a nonprotective mixture of titania and alumina as well as possible nitridation of the substrate alloy.

Acknowledgements

This work was performed in the Framework of the Research Project 2016/23/G/ST5/04128, funded by National Science Centre, Poland. The HT-XRD work was performed in the Framework of the Research Project DFG No. SCHU 1372/6, funded by DFG-Deutsche Forschungsgemeinschaft (German Science Foundation). The authors acknowledge the financial support. The authors thank Mr W. Supernak for performing the cyclic oxidation tests and M. Liśkiewicz for sample preparation using FIB.

Data availability

The raw/processed data required to reproduce these findings cannot be shared at this time as the data also forms part of an ongoing study.

6. Literature

[1] T. Klein, H. Clemens, S. Mayer, Materials 9 (2016) 755.

[2] B.P. Bewlay, S. Nag, A. Suzuki, M.J. Weimer, TiAl Alloys in Commercial Aircraft Engines, Taylor & Francis, 2016.

[3] U. Habel, F. Heutling, K. C., W. Smarsly, G. Das, H. Clemens, Proc. 13th World Conf. Titanium, San Diego, CA, USA, John Wiley Sons, Inc. (2016) 1223–1227.

[4] M.P. Brady, W.J. Brindley, J.L. Smialek, I.E. Locci, JOM 48 (1996) 46–50.

[5] E.A. Loria, Intermetallics 8 (2000) 1339–1345.

[6] G.H. Meier, F.S. Pettit, S. Hu, Le J. Phys. IV 03 (1993) C9-395-C9-402.

[7] F. Dettenwanger, E. Schumann, M. Ruhle, J. Rakowski, G. Meier, Oxid. Met. 50 (1998) 269–307.

[8] M. Schütze, JOM 69 (2017) 2602–2609.

[9] R. Swadźba, K. Marugi, Pyclik, Corros. Sci. 169 (2020) 108617.

[10] J.M. Rakowski, F.S. Pettit, G.H. Meier, F. Dettenwanger, E. Schumann, M. Ruhle, Scr. Metall. Mater. 33 (1995) 997–1003.

[11] N. Zheng, W.J. Quadakkers, A. Gil, H. Nickel, Oxid. Met. 44 (1995) 477–499.

[12] S. Becker, A. Rahmel, M. Schorr, M. Schütze, Oxid. Met. 38 (1992) 425–464.

[13] V. Shemet, H. Hoven, W.J. Quadakkers, Intermetallics 5 (1997) 311–320.

[14] L. Swadzba, G. Moskal, M. Hetmanczyk, B. Mendala, G. Jarczyk, Surf. Coatings Technol. 184 (2004) 93–101.

[15] L. Swadzba, A. Maciejny, B. Mendala, G. Moskal, G. Jarczyk, Surf. Coatings Technol. 165 (2003) 273–280.

[16] N. Laska, R. Braun, Oxid. Met. 81 (2014) 83–93.

[17] R. Braun, M. Fröhlich, W. Braue, C. Leyens, Surf. Coatings Technol. 202 (2007) 676–680.

[18] N. Laska, R. Braun, S. Knittel, Surf. Coatings Technol. 349 (2018) 347–356.

[19] A. Lange, R. Braun, M. Heilmaier, Intermetallics 48 (2014) 19–27.

[20] M. Goral, L. Swadzba, G. Moskal, G. Jarczyk, J. Aguilar, Intermetallics 19 (2011) 744–747.

[21] R. Braun, M. Fröhlich, C. Leyens, D. Renusch, Oxid. Met. 71 (2009) 295–318.

[22] A. Szkliniarz, G. Moskal, W. Szkliniarz, R. Swadźba, Surf. Coatings Technol. 277 (2015).

[23] R. Swadźba, L. Swadźba, B. Mendala, B. Witala, J. Tracz, K. Marugi, Pyclik, Intermetallics 87 (2017) 81–89.

[24] M. Goral, L. Swadzba, G. Moskal, M. Hetmanczyk, T. Tetsui, Intermetallics 17 (2009) 965–967.

[25] A. Donchev, E. Richter, M. Schütze, R. Yankov, J. Alloys Compd. 452 (2008) 7–10.

[26] M. Schütze, G. Schumacher, F. Dettenwanger, U. Hornauer, E. Richter, E. Wieser, W. Möller, Corros. Sci. 44 (2002) 303–318.

[27] S. Friedle, N. Nießen, R. Braun, M. Schütze, Surf. Coatings Technol. 212 (2012) 72–78.

[28] N. Laska, S. Friedle, R. Braun, M. Schütze, Mater. Corros. (2016) 1–10.

[29] S. Taniguchi, A. Andoh, Oxid. Met. 58 (2002) 545–562.

[30] S. Taniguchi, T. Shibata, A. Murakami, Oxid. Met. 41 (1994) 103–113.

[31] S. Taniguchi, Y. Tachikawa, T. Shibata, Mater. Sci. Eng. A 232 (1997) 47–54.

[32] M. Fröhlich, R. Braun, C. Leyens, Surf. Coatings Technol. 201 (2006) 3911–3917.

[33] N. Zheng, W. Fischer, H. Grübmeier, V. Shemet, W.J. Quadakkers, Scr. Metall. Mater.

33 (1995) 47–53.

[34] V. Shemet, A.K. Tyagi, J.S. Becker, P. Lersch, L. Singheiser, W.J. Quadakkers, Oxid. Met. 54 (2000) 211–235.

[35] V. Shemet, P. Karduck, H. Hoven, B. Grushko, W. Fischer, W.J. Quadakkers, Intermetallics 5 (1997) 271–280.

[36] S. Taniguchi, A. Andoh, Oxid. Met. 58 (2002) 545–562.

[37] S. Taniguchi, T. Shibata, S. Sakon, Mater. Sci. Eng. A 198 (1995) 85–90.

[38] M. Kobayashi, M. Yoshihara, R. Tanaka, High Temp. Technol. 8 (1990).

[39] G. Schumacher, F. Dettenwanger, M. Schütze, U. Hornauer, E. Richter, E. Wieser, W. Möller, Intermetallics 7 (1999) 1113–1120.

[40] F. Dettenwanger, E. Schumann, M. Ruhle, J. Rakowski, G. Meier, Oxid. Met. 50 (1998) 269–307.

[41] E.H. Copland, B. Gleeson, D.J. Young, Acta Mater. 47 (1999) 2937–2949.